European Polymer Journal 220 (2024) 113460

Contents lists available at ScienceDirect

European Polymer Journal

journal homepage: www.elsevier.com/locate/europolj

# Polar polyethylene block copolymer synthesis via organometallic-mediated radical polymerization using Co(Salen) complexes

Chenying Zhao, Eva Harth *

*Department of Chemistry, Center of Excellence in Polymer Chemistry, University of Houston, 3585 Cullen Boulevard, Houston, TX 77030, United States*

ARTICLE INFO

*Keywords:*
Organometallic-mediated radical polymerization
Reversible termination
Degenerative transfer
UV-induced radical polymerization

ABSTRACT

We present the synthesis of polar polyethylene block copolymers via organometallic-mediated radical polymerization (OMRP) combining a controlled radical polymerization using Co(Salen) of methyl acrylate (MA), vinyl acetate (VAc) and dimethyl acrylamide (DMA) with a free radical polymerization of ethylene. The use of Co(Salen) allows the polymerization of a broader scope of monomers reaching from less activated monomers (LAM)s to more activated monomers (MAM)s and finally water-soluble, non-ionic monomers via a degenerative transfer mechanism in a living fashion using photoinitiator (2,4,6-trimethylbenzoyldiphenyl) phosphine oxide (TPO) under UV irradiation. Given that the Co(Salen) polymeric dormant species can undergo both degenerative transfer and a reversible termination mechanism, the first segment can act as a radical macroinitiator for the sequential free radical ethylene polymerization. A free radical copolymerization study evaluated the reactivities of the polar monomers and ethylene, as well as the feasibility of a propagation of ethylene from the polar segment, using reaction conditions under 50 bar at 65 °C. The reinitiation efficiency ranged between 60–90 % depending on dormant polymer species. Block copolymers of PMA-*b*-PE, PVAc-*b*-PE, and PDMA-*b*-PE contained on average 0.03 to up to 0. 17$\mathbf{F}_{\text{ethylene}}$ polyethylene.. Microdomain formation and phase separation studies confirmed the formation of block copolymers. Choosing Co(Salen) in combination with light-induced-OMRP offered a viable approach to access valuable polar polyethylene block copolymers in a single type of active species with monomers exhibiting different reactivities towards propagation and activation.

## 1. Introduction

Polyethylene (PE) and polar polymers such as polyacrylates, polyacrylamides, and polyvinyl esters, are materials with a broad application spectrum, and are present in our daily lives in form of coatings, adhesives, tubing, packaging and paints.[1,2] Influencing polymer properties can be achieved by forming copolymers, in which specific comonomers are chosen to change the polarity and function of non-polar polymers.[1,3–10] Block copolymers are particularly appealing among the various types of copolymers because segmented polymers are linked together by covalent bonds, thereby inheriting the properties of each segment.[11–14].

The synthesis of PE-polar block copolymers has been challenging due to significant differences in monomer reactivity.[3,15,16] For example, polar monomers can poison the organometallic catalyst employed for ethylene polymerization, especially early transition metal complexes.[15] Several methods have been developed by our group and others to produce PE-polar block copolymers by combining coordination insertion polymerization of ethylene with several radical polymerization techniques, yielding the PE-*b*-polyacrylates,[17–22] PE-*b*-polystyrene,[19–23] and PE-*b*-polyacrylamide copolymers. However, the preparation of PE-*b*-PVAc copolymers remains challenging when using the less reactive polar monomer such as vinyl acetate.[15] Other strategies to prepare polar PE block copolymers are using ethylene radical polymerization in the presence of either polar macroradical initiators or functional chain transfer agents. For example PMMA-*b*-PE and PEG-*b*-PE copolymers were produced using ethylene radical polymerization, in the presence of PMMA-macromonomers[24] and PEG-RAFT chain transfer agents, respectively[25]. However, only a limited scope of specific macromonomers and chain transfer agents are currently available due to the different reactivity of the monomers and restricts the scope of polar segments to prepare a broad scope of block copolymers.

In this work, it was our goal to design a novel route in which the polar macromonomer is replaced by a dormant macroinitiator with a high chain-end fidelity for different monomer classes, including less activated monomers (LAM)s, more activated monomers (MAM)s and

* Corresponding author.
*E-mail address:* harth@uh.edu (E. Harth).

https://doi.org/10.1016/j.eurpolymj.2024.113460
Received 25 June 2024; Received in revised form 10 September 2024; Accepted 12 September 2024
Available online 14 September 2024

water-soluble monomers. Previous approaches selected very specific controlled radical polymerization (CRP) methods for the polar monomer species which resulted in defined dormant chain end functionalities which limits the monomer scope. In comparison, in OMRP the dormant polymer chain is attached to a Co(III) complex and offers a higher versatility towards different monomer classes.

The homolysis of the carbon–metal bond requires a lower bond dissociation energy (BDE) in the reactivation process in contrast to other CRP techniques.[26–29] The decreased BDE allows for a facile reactivation through reversible termination (RT) but also suppresses the decomposition of the Co(III) species working as a chain transfer agent through a degenerative transfer (DT) mechanism.[28] Another advantage of the observed lower BDE allows the organocobalt complex to participate in ethylene radical polymerization.[30–32] However, a too easily accessible radical species can also result in uncontrolled activation. Overall, several organometallic complexes have been successfully applied in OMRP with polar monomers of different reactivities, such as MA and VAc [28,33,34]. But, $Co(acac)_2$, [33,35,36]which is mainly utilized for the polymerization of VAc shows limited reactivity towards acrylates and acrylamides. On the other hand, the $Co(acac)_2$ catalyst has been reported to facilitate the polymerization of ethylene. In 2015, Detrembleur showed the preparation of a PVAc-*co*-PE copolymer using the $Co(acac)_2$complex.[6] With the ability to undergo the RT mechanism of CRP in OMRP, the PVAc-$Co(acac)_2$ complex was able to act as a radical initiator for ethylene polymerization and a PVAc-*b*-PE block copolymer was produced.[32] As mentioned before, $Co(acac)_2$ has limited effectiveness in preparing the polymeric dormant species of a broad scope of polar monomers. In general, it would be advantageous to explore a mediating catalyst which allows access to a broader monomer scope and is not limited to only one monomers class such as LAMs. [27,37].

(*S,S*)-(+)-*N,N'*-Bis(3,5-di-*tert*-butylsalicylidene)-1,2-cyclohexanediamino cobalt(II), (Co(Salen), is another Co complex which is utilized as a catalyst in OMRP.[38,39] With two oxygen and two nitrogen donors, the low spin Co(Salen) complex and a resulting low spin polymer-Co(Salen) allowed CRP of MA and VAc initiated by Azobisisobutyronitrile (AIBN) at 65℃. Peng and coworkers found through extensive studies that the concentration of radicals, monomers, Co (Salen) and monomer reactivities played critical roles in achieving CRP of both MA and VAc in which DT and RT mechanisms coexist [38]. Fu and coworkers introduced a photoirradiation pathway utilizing diphenyl (2,4,6-trimethylbenzoyl) phosphine oxide (TPO) as the initiator, in which visible light irradiation led to a bond dissociation of the TPO to generate two radical species to initiate the polymer chains[39]. In this fashion, a CRP of acrylates, vinyl esters, and acrylamides was achieved using Co(Salen)[39]. The main factor for the CRP was reasoned by the high control of the radical concentration through the photoirradiation in contrast to the thermal initiation using AIBN. Furthermore, the Co(Salen) mediated radical polymerization was found to involve mainly the DT mechanism.[39] The capability to undergo DT allows the preparation of various dormant species through a CRP process.[39,40] These two reports demonstrate the coexistence of DT and RT in the Co(Salene) mediated CRP. The ability to undergo the RT mechanism enables the dormant species to act as a functionalized radical initiator for polymerization, leading to a functionalized polymer product.[39–41].

This underscores the potential of the Co(Salen) dormant species to serve as both a chain transfer agent in DT and initiator in RT.[39] Taking advantage of the dual nature of polymer-Co(Salen) dormant species, it is thought that the polar-PE block copolymer can be prepared using polymer-Co(Salen) dormant species.

In this work, we propose a synthesis method for polar-PE block copolymers using dormant species from OMRP mediated by Co(Salen). The feasibility of the synthesis of polar-PE block copolymers using polymeric Co(Salen) dormant species initiating ethylene radical polymerization was evaluated. With the broad monomer capabilities of the Co(Salen)-mediated radical polymerization, we demonstrate the synthesis PE-polar block copolymers utilizing different monomer classes, such as LAMs, MAMs and water-soluble monomers.

## 2. Results and discussion

To study the feasibility of preparing polar-PE block copolymers using polymer-Co(Salen) dormant species, an investigation was conducted to mechanistically evaluate possible synthetic routes involving radical polymerization initiation and chain propagation concepts (Scheme 1). This included: (1) polar functionalized macroinitiators generated by OMRP of polar monomers undergoing a degenerative transfer mechanism; (2) macroradical generation involving homolytic bond cleavage of dormant species through the RT mechanism; (3) chain-initiating species requiring an ethylene addition to macroradicals; (4) propagation of non-polar block with ethylene, producing the polar-PE block copolymers.

### 2.1. Synthesis of polymeric Co(Salen) dormant species

To prepare PE-polar block copolymers, a polar functionalized macroinitiator, which is also a polymer dormant species with a high chain end-fidelity, is desired. Radical polymerization driven by OMRP favors resonance stable radical species, to enable reactivation and propagation in the reversible deactivation equilibria. Ethylene monomers do not lead to stabilized radicals due to the lack of a functional group and therefore the preparation of polyethylene dormant species is challenging. Consequently, block copolymer synthesis through the OMRP mechanism is designed from a controlled polymerization of the polar monomer which is then followed by a free radical polymerization of the ethylene monomer. Therefore, we investigated the living polymerization of the chosen polar monomers conducted under OMRP conditions using Co (Salen). We sought to elucidate if Co(Salen) is an ideal catalyst to promote the living polymerizations of LAMs, MAMs and water-soluble monomers by UV irradiation. Both thermal initiation and irradiation initiation were investigated for polymerization of MA, VAc, and DMA, (Scheme 2 and Table S1).

The thermal initiation was achieved using AIBN at 65℃, and resulted in poly(methyl acrylate), (PMA) (Table S1, entry 1) and poly(vinyl acetate) (PVAc) (Table S1, entry 3) with a narrow dispersity ($Đ$) of $< 1.35$). However, poly(*N*, *N*-dimethyl acrylamide) (PDMA), produced from thermal initiation (Table S1, entry 5), showed a $Đ = 1.84$. This higher $Đ$ suggested an uncontrolled radical polymerization with irreversible termination and chain transfer events. This implied limitations of Co (Salen) in mediating controlled radical polymerizations through thermal initiation. Therefore, we investigated a photo-induced initiation using TPO under UV irradiation at a wavelength of 365 nm which is the main

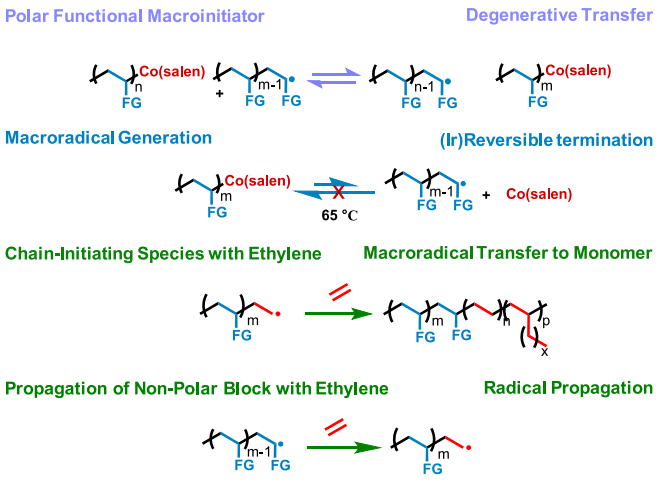


**Scheme 1.** Radical polymerization using polymer-Co(Salen) dormant species.

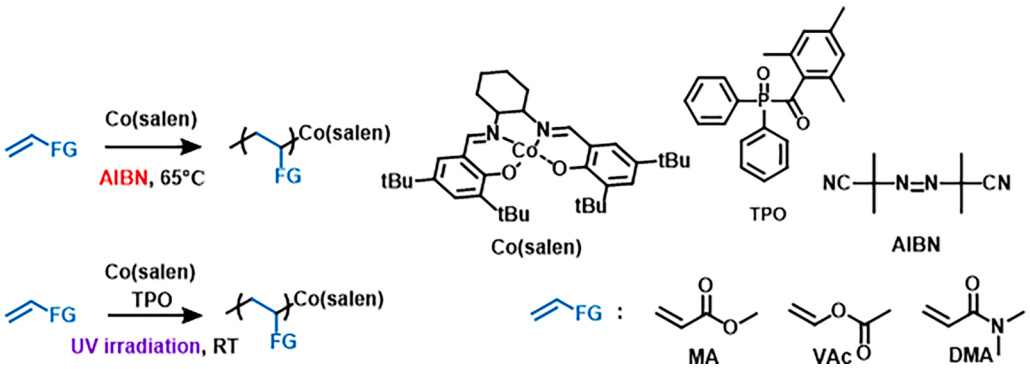


**Scheme 2.** Organometallic mediated radical polymerization using Co(Salen).

absorption wavelength for TPO. In contrast to Fu et al. we did not opt for visible light irradiation at high intensity (3 mW/cm$^2$) which resulted in extended reaction times.[39] Therefore, the polymerization experiments were conducted using a lower light intensity at 1.7 mW/cm$^2$ for MA and VAc. Monomer to initiator to catalyst ratios for PMA ([M]:[TPO]:[Co]) were 100:1:1 and reactions were run in toluene at monomer concentrations of 1 mmol/ml, resulting in PMA with a $Đ$ of 1.14. The same conditions were used for VAc, 175:2:1 ([M]:[TPO]:[Co]) in neat conditions and gave PVAc with a low $Đ$ of 1.32 as shown in Table 1, entries 1 and 2. However, PDMA, produced under identical irradiation conditions, had a $Đ$ = 1.98 and the experimental molecular weight was lower than anticipated (Table S1, entry 6). This suggested a higher degree of propagating radical species than initially expected. To address this issue, the light intensity was reduced from 1.7 mW/cm$^2$ to 0.2 mW/cm$^2$ to decrease the concentration of radicals (Table 1, entry 3). Under these conditions and using ratios of 75:1:1 ([M]:[TPO]:[Co]) the $Đ$ decreased to 1.31. This indicated that controlled radical polymerization is favorably conducted and initiated under UV light.

For a more detailed investigation, kinetic experiments were carried out to determine the living window of MA, VAc, and DMA, using the same irradiation conditions outlined in Table 1, entries 1–3. However, we chose a higher monomer ratio for each of monomers (350:1:1 for MA, 540:1:1 for VAc and 160:1:1 for DMA) to achieve a better understanding of the living window of each polar monomer family in their respective polymerization in the selected conditions (Table 2). Linear relationships were observed between ln([M0]/[Mt]) and reaction times for the polymerization of the respective monomers (MA (Figure S10(a)), VAc (Figure S12(a)), and DMA (Figure S14(a)). These results suggested first-order kinetics indicating CRPs. Furthermore, the $Mn_{exp}$ aligned with conversion in the OMRP process for MA (Figure S10(b)), VAc (Figure S12(b)), and DMA (Figure S14(b)), all with low $Đ$. This kinetic study suggested that controlled radical polymerization was achieved after a reversible deactivation equilibrium was established. Chain-end fidelity is another characteristic of CRP. Therefore, we conducted a propagation resumption experiment to examine the chain-end fidelity of the polar macroinitiators. The propagation resumption was accomplished by (1) interrupting the polymerization by removing the UV irradiation, and (2) resuming the propagation by applying reactivation by both thermal reactivation at 65 °C and UV irradiation only. Samples were collected both before and after the resumption (ON-OFF-ON) for analysis of conversion, molecular weight, and $Đ$ (Fig. 1).

Figure S15 depicts the $^1$H NMR spectrum of the polymer-Co(Salen) dormant species prepared from MA polymerization. The signal detected at 7.96 ppm corresponds to the unreacted photo-initiator, implying that a fraction of the photo-initiator was not activated and did not participate in the initiation of the first block. These initiators could act as radical initiators during the resumption of propagation, leading to a DT mechanism. By switching from UV irradiation to thermal activation as the propagation resumption method, we could prevent the radical initiation from unreacted initiators. Both the RT and DT mechanisms

**Table 2**
Polymerization of monomers mediated by Co(Salen), initiated by TPO under UV irradiation.

| Entry | Monomers | Time (min) | Conversion (%) | $Mn^{theo.}$(g/mol)[a] | $Mn^{exp.}$(g/mol) | $Đ$ |
|---|---|---|---|---|---|---|
| 1 | MA[d] | 30 | 11 | 3,800 | 1,290[b] | 1.08[b] |
| | | 60 | 55 | 18,900 | 16,040[b] | 1.17[b] |
| | | 130 | 85 | 29,200 | 21,360[b] | 1.15[b] |
| 2 | VAc[e] | 60 | 3 | 700 | 3,000[b] | 1.26[b] |
| | | 100 | 16 | 3,700 | 7,400[b] | 1.32[b] |
| | | 130 | 23 | 5,300 | 8,700[b] | 1.39[b] |
| 3 | DMA[f] | 220 | 36 | 5,400 | 5,150[c] | 1.59[c] |
| | | 230 | 48 | 7,100 | 8,000[c] | 1.38[c] |
| | | 300 | 85 | 12,700 | 11,950[c] | 1.32[c] |

[a] Theoretical molecular weight was calculated based on the following equation: $M_n^{theo}$=([M]/[Co(Salen)] × $M_w^M$) × conversion, where [M], [Co(Salen)], and $M_w^M$ correspond to initial monomer concentration, initial Co(Salen) catalyst concentration, and molar mass of the monomer, respectively. [b]Molecular weight ($M_n^{exp}$) and $Đ$ were determined by GPC analysis with sample run in THF at 40°C calibrated to poly(methyl methacrylate) standards. [c]Molecular weight ($M_n^{exp}$) and $Đ$ were determined by GPC analysis with sample run in 10 mM LiBr in DMF at 40°C calibrated to poly(methyl methacrylate) standards. [d][MA]:[TPO]:[Co(Salen)] = 400:1:1, [MA] = 1 mmol/mL in toluene, UV intensity 1.7 mW/cm$^2$. [e][VAc]:[TPO]:[Co(Salen)] = 540:2:1, net reaction., UV intensity 1.7 mW/cm$^2$. [f][DMA]:[TPO]:[Co(Salen)] = 160:1:1, [DMA] = 1 mmol/mL in toluene, UV intensity 1.7 mW/cm$^2$.

**Table 1**
Co(Salen)-mediated radical polymerization using UV initiators for MA, vinyl acetate, and *N,N*-dimethyl acrylamides.

| Entry | Monomer | Initiator | [M](mol/L) | Conversion(%) | $M_n^{theo.}$(g/mol)[a] | $M_n^{exp.}$(g/mol) | $Đ$ |
|---|---|---|---|---|---|---|---|
| 1 | MA | TPO(UV)[c] | 1.0 | 45 | 3,900 | 13,500[b] | 1.14[b] |
| 2 | VAc | TPO(UV) [c] | Bulk | 66 | 5,700 | 6,900[b] | 1.32[b] |
| 3 | DMA | TPO(UV)[e] | 1.0 | 36 | 3,600 | 7,140 [d] | 1.31 [d] |

[a] $M_n^{theo.}$ = ([M] × conversion(%) × Mw)/[Co(Salen)]. Conversion was calculated using $^1$H NMR. Mw corresponding to the molecular weight of monomers. [b]Determined using gel permeation chromatography (GPC) with sample run in THF at 40°C calibrated to poly(methyl methacrylate) standards. [c]Intensity 1.7 mW/cm$^2$. [d]Determined using gel permeation chromatography with sample run in 10 mM LiBr in DMF at 40°C calibrated to poly(methyl methacrylate) standards. [c]Intensity 0.2 mW/cm$^2$.

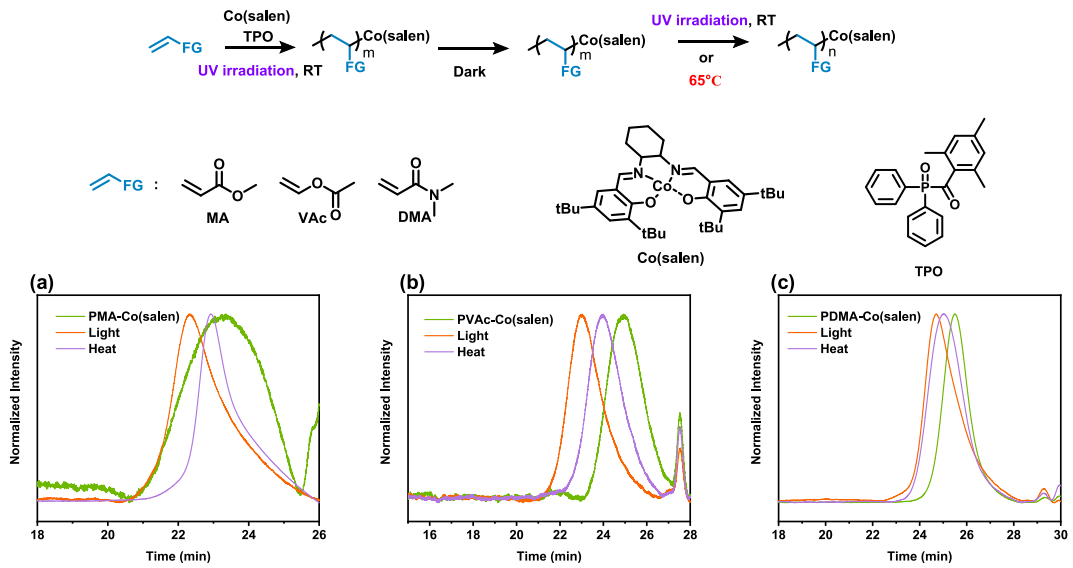


**Fig. 1.** The propagation resumption experiments of polymer-Co(Salen) dormant species by through both UV irradiation and thermal activation. (a) the GPC trace of PMA-Co(Salen) resumed MA polymerization; (b) the GPC trace of PVAc-Co(Salen) resumed VAc polymerization; (c) the GPC trace of PDMA-Co(Salen) resumed DMA polymerization.

have been observed in the Co(Salen)-mediated radical polymerization but dominantly conducted using the DT mechanism.[35,38,42] In the absence of UV light, we hypothesized that all radical species were produced by the homolytic bond cleavage of the polymer-Co(Salen) dormant species. The resumption of propagation was investigated under both thermal reactivation (65℃) and photoirradiation (UV). The reaction was initiated using the same batch of PMA-Co(Salen) dormant species from a Co(Salen)-mediated radical polymerization of MA with a conversion of 27 % (Table S5, entry 1). Following the resumption of propagation, the conversion increased to 68 % via UV irradiation (Table S5, entry 2) and 35 % through thermal reactivation (Table S6, entry 3). Under both UV irradiation and thermal activation, the $Đ$ of the polymer increased, ranging from 1.10 to 1.17 with UV exposure to 1.37 with thermal activation. The UV-irradiated propagation resumption of VAc was carried out for 30 min to prevent polymer precipitation at high conversion. The thermally activated propagation was conducted for 120 min to achieve a reasonable conversion. The PVAc-Co(Salen), used for propagation resumption, was stopped at a conversion rate of 5 % and a $Đ$ of 1.15 (Table S6, entry 1). After 30 min of reaction resumption, the conversion rate increased to 33 % through photo-activated propagation (Table S6, entry 2), while the conversion rate only reached 18 % after a 120-minute resumption at 65℃ (Table S6, entry 3). Therefore, we can conclude that a faster chain propagation resumption is achieved through UV irradiation. Moreover, the $Đ$ did not significantly increase in either case.

The resumption of propagation for dormant PDMA-Co(Salen) species was carried out in the same fashion as for the dormant PMA-Co(Salen) species discussed above. Here, the process began with a Co(Salen)-mediated radical polymerization that had been interrupted by removal of UV irradiation, at a conversion of 58 % (Table S7, entry 1). Upon resuming propagation for the same duration, the conversion rose to 98 % under UV irradiation (Table S7, entry 2) and 95 % under thermal activation (Table S7, entry 3). This suggested that the PDMA-Co(Salen) was reactive in reinitiating chain extension for both RT and DT mechanisms, with the $Đ$ increasing to 1.40 in both cases. The reinitiation of propagation suggested that the dormant polymer-Co(Salen) species, created through OMRP using Co(Salen) and TPO under UV light, maintained high chain-end fidelity and could resume propagation through radical mechanisms. Additionally, given that propagation resumption occurred in all monomer families we investigated, we concluded that the polymer-Co(Salen) dormant species, created through a DT process, could potentially undergo also a RT mechanism and acting as a macroradical initiator.

### 2.1.1. *Monomer reactivity of ethylene*

Prior to conducting an ethylene radical polymerization in the presence of Co(Salen), we first sought to examine the reactivity of the ethylene monomer. Given the high-pressure reactor's requirements for ethylene radical polymerization, the thermal initiation by AIBN at 65 °C was employed, instead of photoinitiation. Dimethyl carbonate (DMC) was chosen as the solvent due to its low chain transfer constant.[43,44] The polymerization process took place in the DMC under 50 bar for a period of 16 h in the absence of Co(Salen). PE was not soluble in the DMC, leading to precipitation during polymerization. The resulting polymer was characterized by $^1$H NMR (Nuclear Magnetic Resonance) (Figure S22). Resonances were detected at 3.78 ppm and 4.16 ppm, corresponding to the chain transfer product by a radical transfer to the solvent. The branching density of the resulting polymer was 81/1000 carbon atoms (Figure S23). The findings indicated that the radical polymerization of ethylene can be conducted at 65 ℃ under 50 bar pressure and is a feasible and practical process.

In another experiment, the radical polymerization of ethylene was conducted in the presence of Co(Salen). Since Co(Salen) was insoluble in DMC, the reaction was carried out in a toluene/DMC (V/V 1:5) mixture. After introducing Co(Salen) into the polymerization, the branching density rose from 81/1000 to 270/1000 carbons (Figure S24). The rise in branching density indicated an increased intermolecular transfer, potentially due to a decrease in radical stability. Additionally, no signals were detected between 4.5–6.0 ppm in $^1$H NMR conducted with/without the Co(Salen) (Figures S22 and S24), ruling out disproportionation termination as a mechanism in this polymerization. Following the introduction of Co(Salen) and toluene, the resonances at 3.78 and 4.16 ppm diminished (Figure S24). In contrast, new resonances appeared at 2.75, 3.00, 3.20, and 4.28 ppm, which correspond to radical chain transfer to both DMC and toluene solvents (Figure S24). Signals were detected at 7.0–7.5 ppm in $^1$H NMR, but these did not match to the signals of the ligand as reported in literature. As Co(Salen) is not detectable in $^1$H NMR, the resonance detected at 7.0–7.5 ppm were attributed to the dormant species of the polymer-Co$^{III}$(Salen).[45] To explore whether the produced PE-Co$^{III}$(Salen) was able to be reactivated, (2,2,6,6-Teramethylpiperidin-1-yl)oxy) TEMPO trapping experiments, and chain extension experiments were conducted separately.

The TEMPO was added at 1 bar as radical scavenger to test the presence of PE macroradicals using the same conditions used for the polar monomer addition experiments and subsequent propagation. A signal at 4.24 ppm was observed after the TEMPO trapping experiment, indicating a potential TEMPO trapping product (Figure S28). However, we expect the protons adjacent to the TEMPO to move upfield to appear around 3.6 ppm. Moreover, the resonances of both the TEMPO compound and PE coincided in the 0.8–1.7 ppm region (Figure S28). This overlap made it challenging to conclusively confirm the presence of a PE-TEMPO product. Additionally, a chain extension experiment was carried out using MA through thermal activation. Here, MA was added under 1 atm of nitrogen atmosphere, and the resulting polymer was purified by precipitation in methanol. Resonances at 3.64 ppm, 2.29 ppm, and 1.4–1.9 ppm in $^{1}$H NMR suggested the formation of PMA (Figure S27). In $^{1}$H DOSY (Diffusion Ordered Spectroscopy), a diffusion coefficient of 58.25 mm$^{2}$/Ms was reported at 3.64 ppm, while a signal at 1.29 ppm reported a diffusion coefficient of 0.2955 m$^{2}$/Gs (Figure S29). The difference in diffusion coefficients indicated that PE-*b*-PMA had not formed, instead two homopolymers had been produced, polymerizing MA under thermal conditions using AIBN at 65 ℃. As a result, the polymer was treated with acetone to remove PMA homopolymer. The resulting material showed only trace amounts of PMA in comparison to PE according to the $^{1}$H NMR (Figure S25) and agreed with the previous assumption that two homopolymers had been formed.

We concluded from these series of experiments that we successfully carried out the radical polymerization of ethylene at a pressure of 50 bar and a temperature of 65℃. This was the case regardless of whether Co (Salen) was present or not. However, the PE-Co(Salen) is not reactive and does not produce a PE-macroradical to be captured or to initiate a propagation reaction with polar monomers. The PE-Co(Salen) did not show any reactivity during the reactivation examination. We suggest that the change of the reaction conditions, in removing the pressure, necessary to add the polar monomer and to conduct a radical polymerization is not beneficial to reactivate the PE-Co(Salen). Therefore, we confirm that a block copolymer synthesis requires to be conducted starting from the polar macromonomer block.

### 2.1.2. Copolymerization of MA, VAc and DMA with ethylene

To test if a chain extension of the polar macroradical species is possible through the addition of ethylene, we sought to investigate the copolymerization of polar monomers with ethylene at 50 bar and 65 °C [46]. Specifically, we examined if ethylene and the polar monomers have a comparable reactivity and radical stability as this is a prerequisite for a successful chain initiating species. When monomers with significantly different reactivities are copolymerized and are incompatible, it does not result in copolymers rather than in the formation of two homopolymers.

The reactivity of MA, VAc, and DMA with ethylene was evaluated by conducting random copolymerization. This was done separately for ethylene with each of the three monomer compounds, MA, VAc, and DMA, respectively. The process was conducted at 65℃, under 50 bar pressure, using AIBN as an initiator. After the polymerization, no unreacted polar monomers were detected in $^{1}$H NMR (Figure S30, S37, S42). The reactions were analyzed for the presence of copolymers and homopolymers. We could show that a PMA copolymer was produced through radical copolymerization with a $\boldsymbol{F}_{\text{ethylene}}$ composition of 0.69. The $^{1}$H DOSY of the crude product showed that the resonances at 3.64 ppm and 1.28 ppm had the same diffusion coefficient, indicating the formation of a copolymer (Fig. 2). Besides, the resonance detected at 1.28 ppm had another diffusion coefficient = 0.10612 m$^{2}$/Gs, indicating the production of homopolymer of PE. After purification through precipitation in hexane and washed with methanol, the analysis of the polymer using $^{1}$H–$^{1}$H COSY (Correlated Spectroscopy) showed a correlated signal at 1.50 ppm and 1.28 ppm which suggested a connection between the methylene of polyethylene and the tertiary carbon of PMA (Figure S34). Moreover, in the $^{1}$H–$^{13}$C HMBC (Heteronuclear Multiple Bond Correlation), the resonances detected at 1.40 ppm, 22 ppm, and 1.40 ppm, 30 ppm confirmed the copolymer molecular structure, indicating that the tertiary carbon of the PMA backbone was directly connected to the PE units (Figure S36). Since the radical reactivity is higher for VAc and DMA, a lower amount of propagating radicals was anticipated to result in an increased PE ratio content. As predicted, the PE percentile of the PE-*co*-PDMA and PVAc-*co*-PE copolymers exceeded that of PMA-*co*-PE. The PE ratio for PE-*co*-polar copolymers can also be determined by using $^{1}$H NMR. The PE percentage in the copolymer was reported as 69 % for PE-*co*-PMA, 93 % for PE-*co*-PVAc, and 92 % for PE-*co*-PDMA. These high PE percentages suggested that the production of chain initiating species of ethylene using the polar macroradical at 50 bar and 65 °C was feasible.

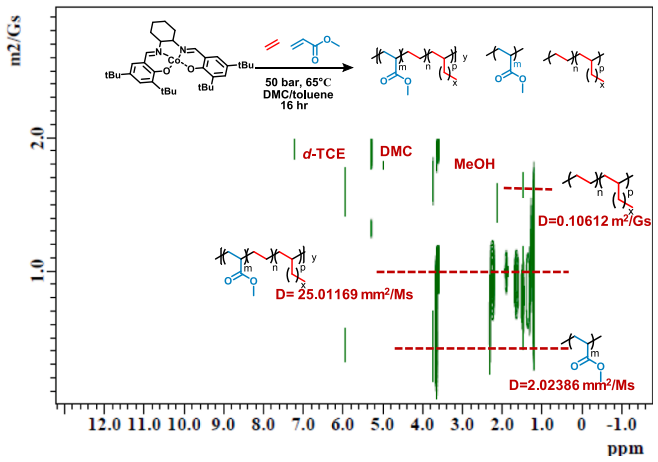


**Fig. 2.** $^{1}$H DOSY of the MA and ethylene copolymerization crude product.

More in detail, the radical copolymerization of VAc and ethylene produced a PE-*co*-PVAc with a $\boldsymbol{F}_{\text{ethylene}}$ composition of 0.93. The formation of this copolymer was confirmed by $^{1}$H DOSY, as the resonance at 4.8 ppm was attributed to PVAc, and 1.32 ppm and 0.86 ppm were attributed to PE, all having the same diffusion coefficient (Figure S38). The proton correlation between the methylene in PE and PVAc was observed in the $^{1}$H–$^{1}$H COSY at 1.32 ppm, 1.48 ppm, indicating the formation of the random copolymer (Figure S39). The $^{1}$H–$^{13}$C HMBC was not performed due to the polymer's low solubility in chloroform, other solvents tested such as tetrachloroethane resulted in shimming difficulties and a low quality of the NMR spectrum.

The radical copolymerization of ethylene and DMA was carried out similarly as above stated for the other monomers leading to a copolymer with a composition of $\boldsymbol{F}_{\text{ethylene}} = 0.92$. According to the $^{1}$H NMR, resonances observed at 0.82 ppm, 1.0–1.8 ppm, 2.6 ppm, and 2.6–3.2 ppm (Figure S44) were attributed to PE and PDMA. According to $^{1}$H DOSY, the resonances ranging from 2.6-3.2 ppm, which represented the dimethyl amide group, and the one at 0.82 ppm, representing the PE methyl group, showed the same diffusion coefficient, suggesting the formation of copolymers (Figure S43). Notably, the methylene on the backbone of both PE and PDMA were detected at 1.0–1.8 ppm. According to the $^{1}$H–$^{13}$C HMBC, the proton at 1.3 ppm is correlated to the carbon at 40 ppm, which belongs to the tertiary carbon of the PDMA backbone (Figure S47). Additionally, the proton detected around 1.2 ppm is correlated to the carbon at 30 ppm, which is identified as the resonance of PE. Therefore, we could conclude that a random copolymer of PDMA was produced.

In addition to NMR analysis, the thermal analysis using thermogravimetric (TGA) and differential scanning calorimetry (DSC) was conducted. The decomposition temperature of PE produced under 50 bar at 65℃ was recorded at 455℃ (Figure S180). A gradient weight loss was observed for PMA-*co*-PE copolymers with an initial decomposition temperature at 360℃ and decomposition temperature at 404℃, which

is lower than the decomposition temperature of PE prepared by free radical polymerization at 454℃ (Figure S182). Only one decomposition state was observed. The TGA of PVAc-*co*-PE and PDMA-*co*-PE copolymers were analyzed in the same fashion. Interestingly, two stages of decomposition were observed for PVAc-*co*-PE. The decomposition of PVAc-*co*-PE copolymer was reported with initial decomposition temperature at 324℃ and decomposition temperature at 365℃ for PVAc segments, and initial decomposition temperature at 426℃ and decomposition temperature at 450℃ for PE segments, which were lower than the decomposition temperature of the prepared PE, suggesting the formation of random copolymers (Figure S181).

The decomposition of PDMA-*co*-PE copolymer was observed with decomposition temperature at 287℃ and 430℃ for PDMA and PE correspondingly (Figure S183). According to the DSC, the melting point ($T_m$) was observed at 112℃ for PE, 101℃ for PMA-*co*-PE copolymer, 92℃ for PVAc-*co*-PE copolymer, and 103℃ for PDMA-*co*-PE copolymer (Figures S187-190). The overall decrease in melting temperature of PE in all copolymer samples suggested a change in composition, therefore effecting the crystallinity of the PE units. Moreover, a decrease in the $T_g$ of the polar units was observed comparing to literature reports of the homopolymers[47–49] suggesting the chain length of the polar segments decreased due to the ethylene incorporation. Taken the NMR characterization and thermal analysis together, they validated the formation of polar-PE random copolymers through the free radical copolymerization. Furthermore, this study has shown that chain propagation, by adding an ethylene monomer, can be achieved while the macroradical reactivity is changed form a more stable to a less stable macroradical when propagating ethylene in a copolymerization process with MA, VAc and DMA.

### 2.1.3. *Reactivity of polymeric dormant species*

When analyzing the mechanism of OMRP mediated by Co(Salen), [39] both RT and DT mechanisms can exist simultaneously as stated previously. The radical species produced by the RT mechanism does not only lead to radical propagation but also to DT to another dormant species (Scheme 3). Both the Poli and Matyjaszewski group reported that an electron donor, such a Lewis base in form of pyridine can potentially coordinate with the cobalt catalyst. [50] A pyridine-coordinated cobalt complex prevents a DT mechanism and is shifting the chemical equilibrium of RT towards polar macroradicals [50].

To evaluate the efficiency of the dormant species to generate radical species, we introduced TEMPO into the system to capture the produced radicals competing with the DT process. As the homolytic cleavage of the TEMPO-polymer species can occur only above 100 °C, we assumed that no reactivation of the captured species will occur at 65 °C, which is the temperature we use for the TEMPO trapping and thermally driven

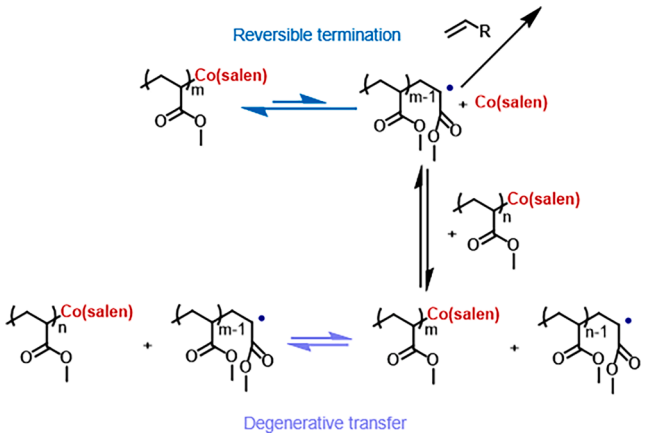


**Scheme 3.** The reversible termination and degenerative transfer mechanisms in the Co(Salen)-mediated radical polymerization of methyl acrylate.

chain extension. Initial TEMPO trapping experiments were conducted to demonstrate the reactivity of the polymer-Co(Salen) dormant species initiating radical species through homolytic cleavage depicted in Fig. 3. Fig. 3 shows the conversion vs. time during the TEMPO trapping experiments. The conversion increased with increased reaction time, suggesting the homolytic bond cleavage of the Co-C bond is time dependent. The conversion of the TEMPO trapping experiments did not reach 100 % after 72 h for the PMA-Co(Salen), PVAc-Co(Salen), and PDMA-Co(Salen) dormant species. This suggested that a portion of the dormant species was incapable of undergoing homolytic bond cleavage.

Therefore, an electron donor, here we selected pyridine, was introduced to the TEMPO trapping experiments. Fig. 3 presents the conversion of TEMPO trapping experiments of the PMA-Co(Salen), PVAc-Co (Salen), and PDMA-Co(Salen) dormant species with/without the Lewis base correspondingly. For the PMA-Co(Salen) TEMPO trapping experiments (Table S8), as the reaction time extended, the conversion of TEMPO trapped PMA steadily increased. It rose from 49 % to 70 % in the presence of pyridine and 34 % to 47 % in its absence. Over 30 % of dormant species underwent homolytic cleavage within 24 h. The reactivation of the dormant species continued after 24 h but at a slower rate, with about an 10 % increase every 24 h when pyridine was present. Without pyridine, the TEMPO trapping conversion rates at 24, 48, and 72 h were 34%, 43 %, and 47 % respectively, displaying a decreasing rate. These results suggested that pyridine facilitated the reactivation of the dormant species through a RT mechanism and that this reactivation was a time-dependent process.

For the PVAc-Co(Salen) dormant species TEMPO trapping experiments (Table S9), the conversion increased as the reaction time extended from 24 to 72 h, similarly to the behavior of the PMA-Co (Salen) dormant species. In the TEMPO trapping experiment, a conversion of 63 % was achieved after 24 h with pyridine, while 46 % without pyridine. With pyridine, the conversion rate increased from 63 % to 74 % between 24 and 48 h but only rose by 5 % from 48 to 72 h. However, without pyridine, the conversion rate had a steady 10 % increase every 24 h from 48 to 72 h. Overall, the conversion with pyridine was consistently higher than without pyridine, suggesting that pyridine accelerated the radical production from dormant species and suppresses the DT mechanism. Furthermore, Fig. 3C and Table S10 document the TEMPO trapping experiments of PDMA-Co(Salen) dormant species in the same fashion as for the other two dormant species. After 24 h of reaction, the conversion reached 81 % with pyridine and 74 % without it. The conversion continued to increase steadily from 48 to 72 h, both with and without pyridine. After 72 h, the conversion rate was 94 % in the presence of pyridine, and 92 % without it. These conversion rates suggested that most of the dormant species undergo homolytic bond cleavage, with the resulting radical being captured by TEMPO. Within the same time duration, the conversion rate was always higher in the presence of pyridine compared to without pyridine.

Overall, when comparing the conversion results between the PMA-Co(Salen), PVAc-Co(Salen), and PDMA-Co(Salen) dormant species, PMA-Co(Salen) demonstrated the lowest conversion. This suggested a higher bond dissociation energy due to the electron-withdrawing group. Conversely, PDMA-Co(Salen) showed the highest conversion, implying rapid dissociation. This aligned with our previous studies indicating that Co(Salen) could not mediate the controlled radical polymerization of DMA at 65℃ and is only possible through photoinduction. The TEMPO trapping experiment revealed the reactivity of the polymer-Co(Salen) dormant species, confirming that the activation through RT was not immediate and was time-dependent. To increase the proportion of dormant species that reactivate, adding pyridine and extending the reaction time are beneficial.

## 2.2. *Synthesis of PMA-b-PE copolymers using PMA-Co(Salen) dormant species*

According to the previous studies, investigating the preparation of

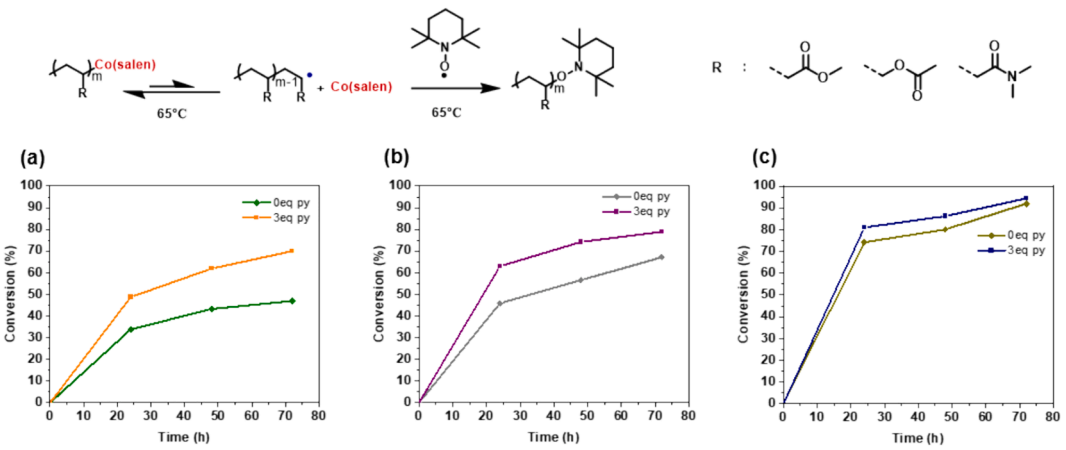


**Fig. 3.** (a) Conversion vs. time of TEMPO trapping experiments of PMA-Co(Salen) dormant species. (b) Conversion vs. time of TEMPO trapping experiments of PVAc-Co(Salen) dormant species. (c) Conversion vs. time of TEMPO trapping experiments of PDMA-Co(Salen) dormant species.

dormant species and reactivity examination of monomers, the reactivity of dormant species as radical initiator and their feasibility in initiating the ethylene polymerization was evaluated. The TEMPO trapping experiments revealed the reactivation behavior of polymeric dormant species. Guided by the previous studies, the preparation of a PMA-*b*-PE copolymer was carried out in consideration of three factors: reaction time, electron donor addition and ethylene pressure.

Scheme 4 illustrates the preparation of PE-based polar block copolymers using polymeric dormant species. Here, we used a range of PMA-Co(Salen) precursors with MW ranging from around 3–5,5 kg/mol. The chain extension was conducted from 48 to 72 h under 50–60 bar with and without the addition of pyridine. The effect of the electron donor, time and pressure was evaluated for the block copolymer preparation. The polymers were characterized by $^{1}$H NMR, $^{1}$H DOSY, and GPC-THF (Figure S86-115). $^{1}$H DOSY was performed for both the dormant PMA-Co(Salen) species and the purified PMA-*b*-PE block copolymers (Fig. 5a). After chain extension, the signals detected at 1.20–1.30 ppm, which belong to the methylene of PE units exhibited the same diffusion coefficient as the signal around 3.5–3.7 ppm. The signal around 3.5–3.7 ppm corresponded to the methoxy group in PMA, implying the formation of the PMA-*b*-PE copolymers. According to the GPC-THF, a decrease in retention time was observed after the chain extension. This suggested an increase in the hydrodynamic volume, indicating that the molecular weight increased, and the composition changed. The formation of the PMA-*b*-PE copolymer was confirmed, according to the $^{1}$H DOSY and GPC-THF characterization. The degree of polymerization (DP) of PE was calculated using the integral of the initiation group and PE in the $^{1}$H NMR. This calculation assumes that all PMA-Co(Salen) dormant species were reactivated and initiated the radical polymerization of ethylene. Therefore, the increase in DP implies a higher radical amount.

Due to the significant polarity difference between poly(methyl acrylate) and PE, a phase separation was anticipated. This phenomenon was analyzed by small angle x-ray scattering (SAXS) (Fig. 4). Though the DP of PE was low, a scattering signal was detected and provided evidence of phase separation and microdomain formation proving the presence of block copolymers. An increased PE ratio leads to a more significant scattering signal as can be observed in Figure S84 compared to Figure S85. This observation further confirmed that different PMA-b-PE compositions led to the formation of microdomains. In comparison to the PMA-*co*-PE copolymers, two stages of decomposition were observed in TGA of PMA-*b*-PE copolymers (Table 3, entry 3). The PMA segment decomposed at 370°C and the PE segment decomposed at 449°C (Figure S184). The two significant decompostion stages alinged with the decompostion temperatures of the individual homopolymers. This observation further confirmed the formation of block copolymers. Besides, a *T*m = 109°C and *T*g = 3°C was observed in DSC analysis, which agreed with previous results of PE, validating the existence of the diblock copolymer segments (Figure S187, S191).

By comparing entries 1 and 3, and entries 2 and 4 in Table 3, the DP of PE increased from 4 to 5 when the reaction time was extended from 48 to 72 h, regardless of the presence of an electron donor. The reduction of the retention time and increased molecular weight was observed in the GPC-THF trace suggesting the increase of the molecular weight and polymer composition change. This observation aligned with results of the PMA-Co(Salen) dormant species TEMPO trapping experiments, which concluded that the reactivation of the PMA-Co(Salen) dormant species was a time-dependent process. Extended reaction times result in the production of more radical species over time.

Table 3, entries 1, 2, 5, and 6, show the results of the PMA-*b*-PE copolymer prepared under 50 bar and 60 bar ethylene pressure. An increase in ethylene pressure was expected to raise the reactivity of ethylene and DP. As anticipated, an increase in DP was observed, from 4 to 4.5 without the electron donor and 6 to 6.5 with the pyridine. However, the increase was minor because the pressure remained low compared to industrial standards. The influence of the electron donor,

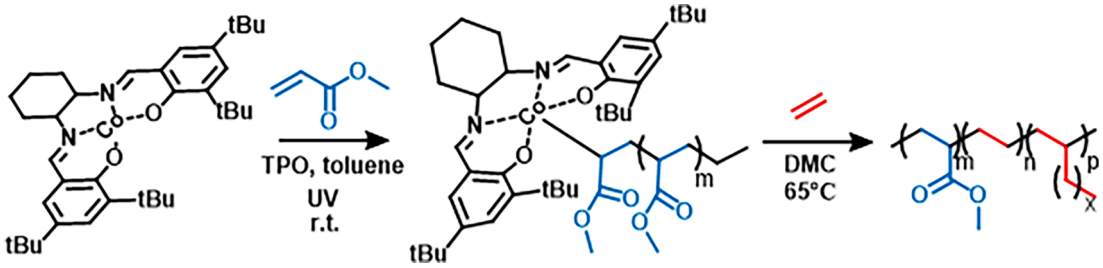


**Scheme 4.** Synthesis of PMA-*b*-PE copolymers using PMA-Co(Salen) dormant species.

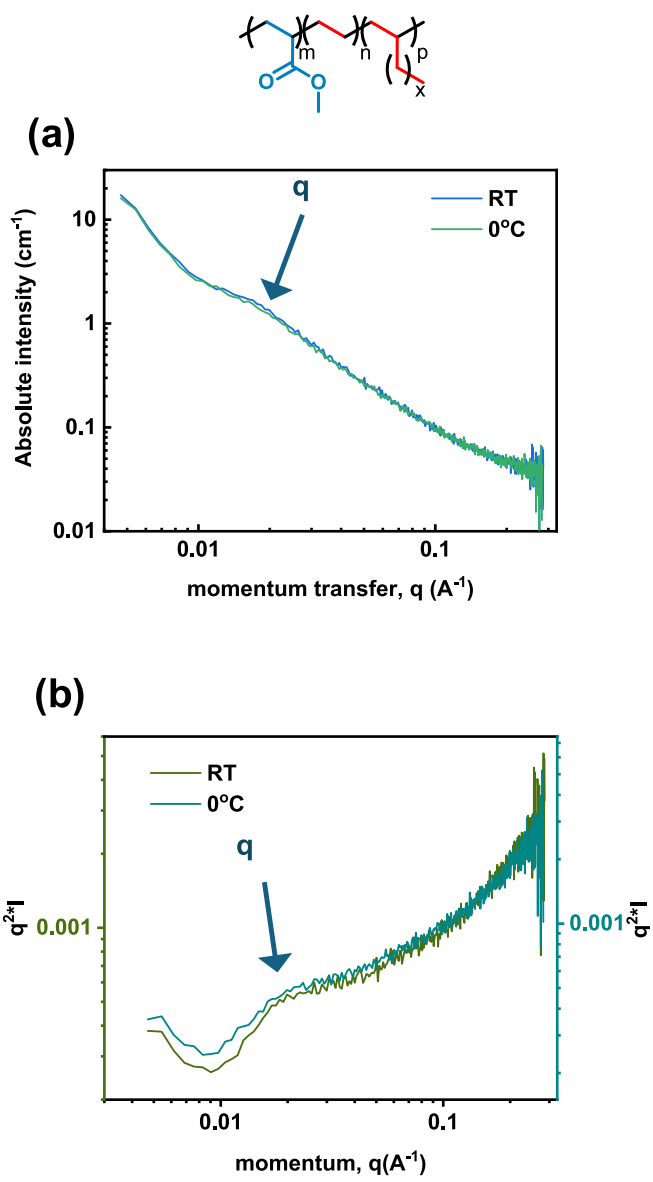


**Fig. 4.** SAXS of PMA-*b*-PE copolymer (Table 3, entry 3) at 0 °C and room temperature. (a) Absolute intensity(I) vs. momentum transfer(q); (b) q2I vs. momentum transfer(q).

pyridine, was examined in this study as well. It coordinated to the Co (Salen), and an increased ratio of the PMA-Co(Salen) dormant species was activated. We anticipated more PE to be produced as the number of macroradicals increased. The electron donor's impact was evaluated under varying reaction durations and pressures. Comparing entries 1 and 2, 3 and 4, as well as 5 and 6 from Table 3, we observed the DP of PE increased from 4 to 6, 5 to 7.5, and 8 to 9, respectively. Furthermore, extending the reaction time and increasing the ethylene pressure resulted in a higher DP of PE, similar to chain extensions without an electron donor. The ethylene radical chain extension followed the same pattern, regardless of the presence or absence of an electron donor. In addition, the $DP^{cal.}$(PE) was calibrated using the conversion of PMA-Co (Salen) TEMPO trapping experiments to extrapolate the DP of PE with full reactivation and chain extension. After the calibration, the difference in the DP of PE with the same reaction time, reaction pressure and addition of electron donors was significantly reduced and the $DP^{cal.}$(PE) was around 10 (Table 3, entries 1–4). This observation was in agreement with the previous finding that the reaction time and electron donor leading to the increase of dormant species reactivated and initiating propagation.

### 2.3. Synthesis of PVAc-b-PE copolymers using PVAc-Co(Salen) dormant species

The PVAc-*b*-PE copolymer was prepared from the ethylene radical chain extension of the PVAc-Co(Salen) dormant species (Scheme 5). These PVAc-Co(Salen) dormant species were prepared by the Co(Salen) mediated radical polymerization of VAc. The dormant species' reactivity in propagation initiation, the radical transfer to the ethylene monomer, and the ethylene radical polymerization were discussed in previous sections.

The polymers were characterized using $^1$H NMR, $^1$H DOSY, and GPC-THF (Figure S118-147). Both the dormant PVAc-Co(Salen) species and the resulting PVAc-*b*-PE copolymer were analyzed with $^1$H DOSY (Fig. 5b). Signals around 1.1–1.3 ppm were detected prior to chain extension, overlapping with the protons of ethylene units (Figure S 118). The resonance at 1.1–1.3 ppm shared the same diffusion coefficient as the resonance at 4.86 ppm, associated with the tertiary carbon of PVAc. These resonances matched the reported *t*-butyl group of the Co(Salen) species bonded to the PVAc.[39] Following the chain extension, there was a decrease in the signal intensity at 1.1–1.3 ppm, coupled with multiple protons, resulting in a broadened peak. The resonances at 1.24 and 4.86 ppm maintained the same diffusion coefficient, indicating the formation of a polymer containing both ethylene and acetylated units (Figure S121). This implied the presence of a polymeric block structure. Further characterization of the polymer materials was performed by using GPC-THF. The shift in retention time indicated an increase in hydrodynamic volume and changes in polymer composition, suggesting the formation of block copolymers. According to the SAXS analysis

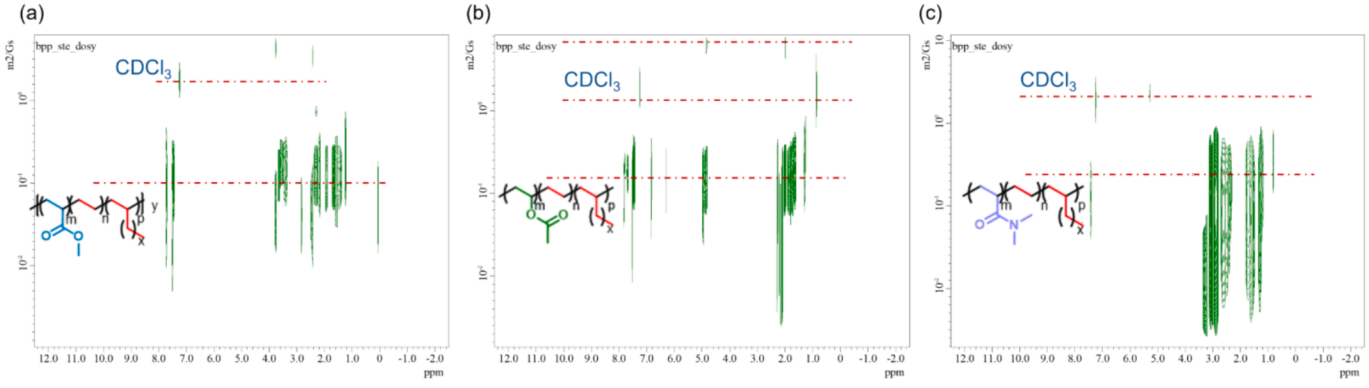


**Fig. 5.** 1H-DOSY of polar PE block copolymers. (a) PMA-b-PE copolymer, (b) PVAc-b-PE copolymer, (c) PDMA-b-PE copolymer.

**Table 3**
PMA-*b*-PE block copolymer by ethylene radical chain extension using PMA-Co(Salen) dormant species.

| Entry | $Mn_{theo.}^{PMA}$ (g/mol)[a] | $Mn_{exp.}^{PMA}$ (g/mol)[b] | Đ [b] | [Py]: [$Co^{II}$] | Pressure (bar) | Time (hr) | DP (PE) [c] | $DP^{cal.}$(PE)[d] | $Mn_{exp.}^{PMA-PE}$ (g/mol)[b] | *Đ* [b] |
|---|---|---|---|---|---|---|---|---|---|---|
| 1 | 2,800 | 4,330 | 1.23 | 0 | 50 | 48 | 4 | 9.0 ± 0.3 | 4,690 | 1.24 |
| 2 | 3,300 | 5,560 | 1.25 | 3 | 50 | 48 | 6 | 9.8 ± 0.4 | 6,780 | 1.21 |
| 3 | 3,200 | 4,630 | 1.15 | 0 | 50 | 72 | 5 | 10.5 ± 0.2 | 5,810 | 1.15 |
| 4 | 2,600 | 3,420 | 1.32 | 3 | 50 | 72 | 7.5 | 10.7 ± 0.8 | 5,500 | 1.26 |
| 5 | 3,800 | 4,430 | 1.25 | 0 | 60 | 48 | 4.5 | 10.5 ± 0.4 | 5,090 | 1.20 |
| 6 | 1,600 | 2,900 | 1.16 | 3 | 60 | 48 | 6.5 | 10.5 ± 0.04 | 3,630 | 1.18 |

[a] The theoretical molecular weight was calculated based on the following equation: $M_n^{theo.\ PMA} = ([M]_0/[Co(Salen)] \times Mw^{MA}) \times$ poly(methyl acrylate) conversion, where $[M]_0$, [Co(Salen)], and $Mw^{MA}$ correspond to initial monomer concentration, initial Co(Salen) catalyst concentration, and molar mass of the MA, respectively. [b]The experimental molecular weight($Mn_{exp}$) and *Đ*) were determined by GPC analysis with samples run in THF at 40℃ calibrated to poly(methyl methacrylate) standards. [c]The DP(PE) was calculated based on the following equation: DP(PE) = (Integral (0.8–1.3 ppm)/4)/(Integral (6.6–6.8 ppm)/2 + Integral(7.5–7.8 ppm)/4). [d]The $DP^{cal.}$(PE) was calculated from DP(PE) following the equation $DP^{cal.}$(PE) = DP(PE) ÷ Conversion. The Conversion was the average conversion from the PMA-Co (Salen) TEMPO trapping experiments (Table S8). The error was calculated from the difference between 2 experiments runs of TEMPO trapping experiments.

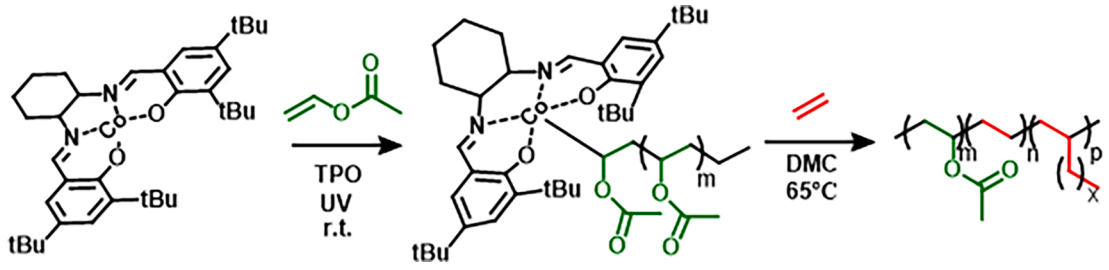


**Scheme 5.** Synthesis of PVAc-*b*-PE copolymers using PMA-Co(Salen) dormant species.

(Figure S116 and S117), scattering was observed for both above and below the $T_g$, suggesting the phase separation and microdomain formation of the polymer segments. This separation indicated the production of block copolymers due to the differing properties of PVAc and PE. When comparing Figure S117 with Figure S116, it was apparent that an increased percentage of PE promoted the phase separation behavior. This demonstrated that although the produced polyethylene segment contained a limited number of repeating units the PVAc-*b*-PE copolymer led to phase separation. Two stages of decomposition were observed in the TGA for PVAc-*b*-PE copolymer (Table 4, entry 4) with decreased decomposition temperature at 338℃ of PVAc and increased decomposition temperature of PE at 449℃ (Figure S185) in comparison to the TGA analysis of PVAc-*co*-PE copolymers. This suggested a more defined structure of each polymeric segment as the decomposition temperature of the PE segment aligns with PE homopolymers. The observation of two significant decomposition stages further confirmed the formation of block copolymers. However, no crystallinity was observed for the PE segments according to the DSC analysis due to the short chain length of PE segments (Figure S192).

The chain extension from the PVAc-Co(Salen) dormant species was investigated in the same fashion as demonstrated for PMA-*b*-PE in which the pressure, reaction duration and the addition of pyridine plays an important role. Table 4 shows the PVAc-*b*-PE copolymers prepared by the ethylene propagation using PVAc-Co(Salen) dormant species. The DP of PE was calculated using $^1$H NMR, based on the assumption that all PVAc-Co(Salen) dormant species underwent ethylene radical polymerization. However, as the TEMPO trapping experiments have demonstrated, a portion of the dormant species is not reactivated during the reaction duration, for PVAc-Co-(Salen) it is 20 % in the presence of pyridine.

As the reaction time increased (entries 1 to 4, Table 4), the DP of PE increased too. This suggested an increased production of PE, regardless of the presence of electron donors. The DP of PE increased from 2.0 to 3.3 without the electron donor, and from 3.4 to 5.3 in its presence. This finding was consistent with the results from the TEMPO trapping experiments. As the reaction time increased, more radical species were generated from the PVAc-Co(Salen) dormant species, leading to increased propagation of ethylene. Ethylene pressures of 50 and 60bars were utilized in this study (as shown in Table 4, entries 1, 2, 5, and 6). It was hypothesized that an increase in pressure would enhance ethylene reactivity through radical polymerization, thereby increasing the DP of PE. As anticipated, the DP rose from 2.0 to 2.4 without the presence of an electron donor and from 3.4 to 3.8 when an electron donor was present. Consequently, the increase in ethylene pressure did increase

**Table 4**
PVAc-*b*-PE block copolymer by ethylene radical chain extension using PVAc-Co(Salen) dormant species.

| Entry | $Mn_{theo.}^{PVAc}$(g/mol) [a] | $Mn_{exp.}^{PVAc}$(g/mol)[b] | Đ [b] | [Py]:[$Co^{II}$] | Pressure(bar) | Time(hr) | DP (PE) [c] | $DP^{cal.}$(PE)[d] | $Mn_{exp.}^{PVAc-b-PE}$(g/mol) [b] | *Đ* [b] |
|---|---|---|---|---|---|---|---|---|---|---|
| 1 | 3,500 | 3,320 | 1.30 | 0 | 50 | 48 | 2.0 | 3.5 ± 0.07 | 3,500 | 1.37 |
| 2 | 2,700 | 2,960 | 1.36 | 3 | 50 | 48 | 3.4 | 4.6 ± 0.09 | 3,220 | 1.33 |
| 3 | 4,400 | 6,090 | 1.32 | 0 | 50 | 72 | 3.3 | 4.9 ± 0.12 | 6,530 | 1.28 |
| 4 | 3,900 | 3,750 | 1.20 | 3 | 50 | 72 | 5.3 | 6.7 ± 0.06 | 3,900 | 1.28 |
| 5 | 2,400 | 2,640 | 1.37 | 0 | 60 | 48 | 2.4 | 4.2 ± 0.08 | 3,340 | 1.27 |
| 6 | 3,800 | 3,410 | 1.28 | 3 | 60 | 48 | 3.8 | 5.1 ± 0.10 | 3,560 | 1.25 |

[a] The theoretical molecular weight was calculated based on the following equation: $M_n^{theo.\ PVAc} = ([M]_0/[Co(Salen)] \times Mw^{VAc}) \times$ poly(vinyl acetate) conversion, where $[M]_0$, [Co(Salen)], and $Mw^{VAc}$ correspond to initial monomer concentration, initial Co(Salen) catalyst concentration, and molar mass of the VAc, respectively. [b]The experimental molecular weight($Mn_{exp}$) and *Đ*) were determined by GPC analysis with samples run in THF at 40℃ calibrated to poly(methyl methacrylate) standards. [c]The DP(PE) was calculated based on the following equation: DP(PE) = (Integral (0.8–1.3 ppm)/4)/(Integral (6.6–6.8 ppm)/2 + Integral(7.5–7.8 ppm)/4). [d]The $DP^{cal.}$(PE) was calculated from DP(PE) following the equation $DP^{cal.}$(PE) = DP(PE) ÷ Conversion. The Conversion was the average conversion from the PVAc-Co (Salen) TEMPO trapping experiments (Table S9). The error was calculated from the difference between 2 experiments runs of TEMPO trapping experiments.

ethylene propagation.

The electron donor was introduced to the system using all the previous conditions of ethylene pressures and reaction times. An expected increase in the DP of PE was observed under each reaction condition. With the presence of the electron donor, the DP of PE increased from 2.0 to 3.4 under 50 bar for 48 h, from 2.4 to 3.8 under 60 bar for 72 h, and from 3.3 to 5.4 under 50 bar for 72 h. These results suggested that the electron donor could enhance the reactivity of the PVAc-Co(Salen) dormant species and lead to an improvement in the propagation of PE starting from the PVAc-Co(Salen) dormant species.

Similar to PMA-*b*-PE copolymer preparation, the $DP^{cal.}$(PE) was calibrated using the TEMPO trapping experiments of PVAc-Co(Salen) to extrapolate the DP of PE with full reactivation and chain extension. Different from PMA-*b*-PE copolymer preparation, the increase in $DP^{cal.}$PE accompanied with increased reaction time, addition of electron donor, and increased ethylene pressure was observed, which indicated that not all initiated dormant species participated in ethylene propagation. This could be caused by the fast reactivation of dormant species leading to irreversible termination. This outcome aligned with the TEMPO trapping experiments in which over 55 % dormant species reactivated within 48 h. Overall, the difference in the DP of PE with the reaction time, reaction pressure was reduced (Table 4, entries 1–4).

### 2.4. Synthesis of PDMA-b-PE copolymers using PDMA-Co(Salen) dormant species

The PDMA-*b*-PE copolymer was prepared by the chain extension of the PDMA-Co(Salen) dormant species (Scheme 6) with ethylene. As for the previous blocks with the other monomer classes, the resulting polymers were subjected to analysis utilizing $^1$H NMR, $^1$H DOSY, and GPC-THF (Figure S150-179). Both the dormant PDMA-Co(Salen) species and the resulting PDMA-*b*-PE copolymer were examined with $^1$H DOSY (Figures S151 and S152). Notably, the methylene proton along the PDMA displayed in the $^1$H NMR at 1.20—1.85 ppm (Figure S150), coincided with the methylene proton of the polyethylene. The signal detected at 1.1–1.3 ppm consistently exhibited the same diffusion coefficient as the signal discerned at 2.6–3.2 ppm, which was attributed to the dimethyl group of the amide (Fig. 5c). The corresponding signals added complexity to the determination of whether the PDMA-*b*-PE copolymer was produced. However, according to the GPC-DMF, the retention time decreased post-chain extension, indicating an increase in MW and alterations in composition. Figure S148 and S149 depicted the SAXS analysis of the PDMA-*b*-PE copolymers. In Figure S148, the scattering was minor at both temperatures, this phenomenon could be attributed to the minimal PE incorporation. In contrast, Figure S149 presented a noticeable scattering signal at room temperature, suggesting phase separation due to block copolymer formation. The scattering was observed at room temperature, and it became less significant when the temperature rose above the $T_g$ temperature of the PDMA homopolymer. The underlying cause of this phenomenon remains to be elucidated. In the TGA analysis, only one stage of decomposition was observed for PVAc-*b*-PE copolymer (Table 5, entry 4) due to the decomposition of PDMA and PE which decomposed at the same temperature at 437℃ (Figure S186). The change in decomposition behavior suggested the formation of block copolymers. The TGA, GPC-DMF and SAXS findings collectively implied the production of PDMA-*b*-PE copolymers.

The DP of PE was calculated based on the assumption that all PDMA-Co(Salen) reactivated and initiated the ethylene radical polymerization. But as previously stated, we also calculated the DP by taking the re-initiation efficiency into consideration. Because methylene along the polyacrylamide backbone and PE overlaps in the 1.1–1.9 ppm range in the $^1$H NMR. The proton integral of the PE segments was calculated by subtracting the proton of methylene of PDMA from the integral of proton shown in the 0.8–1.85 ppm range. The proton integral of the methylene of PDMA was calculated as 2/7 of the proton integral from 1.85 to 3.5 ppm, which belonged to the proton of the dimethyl group and the proton of tertiary along the polyacrylamide backbone.

Table 5 presented the PDMA-*b*-PE copolymers prepared using PDMA-Co(Salen) dormant species and propagation with ethylene. By increasing the reaction time from 48 h to 72 h, the DP of PE increased from 3.7 to 5.9 without electron donor, and 3.8 to 7.2 in the presence of electron donors. This implies that with increased reaction time, the ethylene propagation increased with more dormant species getting activated and initiating the radical propagation, which met our expectations and aligned with the previous reactivity studies. With increased pressure, a slight increase was observed, and the DP increased from 3.7 to 3.9 in the absence of pyridine and 3.8 to 4.8 with the electron donor by increasing the ethylene pressure from 50 bar to 60 bar which remained low compared to industrial standards (400–2500 bar). The change in DP of PE was minor but indicated the trend that the increasing ethylene pressure could produce longer PE segments as the reactivity of ethylene increased.

The impact of the electron donor was investigated across varying reaction times and ethylene pressures. When compared to the polymer created without the electron donor, introducing pyridine to the system after 48 h under 50 bars did not create a significant difference. Nonetheless, as the reaction time increased, this distinction became more noticeable. This aligns with the observed resumption of the propagation study (Table 5, entries 1 and 2). The inclusion of pyridine, acting as the electron donor, elevated the DP of PE from 5.9 to 7.2 at 50 bar over 72 h (Table 5, entries 3 and 4), and from 3.9 to 4.8 at 60 bars over 48 h (Table 5, entries 5 and 6). This raise indicates that the production of PE increased after the addition of the electron donor, activating more dormant species and initiating propagation. This suggests that the electron donor could also stimulate the reactivation of the dormant PDMA-Co(Salen) species.

The $DP^{cal.}$(PE) was calibrated using the conversion of PDMA-Co (Salen) TEMPO trapping experiments to extrapolate the DP of PE with full reactivation and chain extension. Similar to PVAc-*b*-PE copolymer preparation, the increase in $DP^{cal.}$PE was accompanied with increased reaction time, the addition of the electron donor, and increased ethylene pressure, which indicated that not all initiated dormant species participated in the ethylene propagation. This could be caused by the fast reactivation of dormant species leading to irreversible termination, which aligned with the TEMPO trapping experiments that over 80 % dorant specieces reactivated within 48 h, which agreed with the

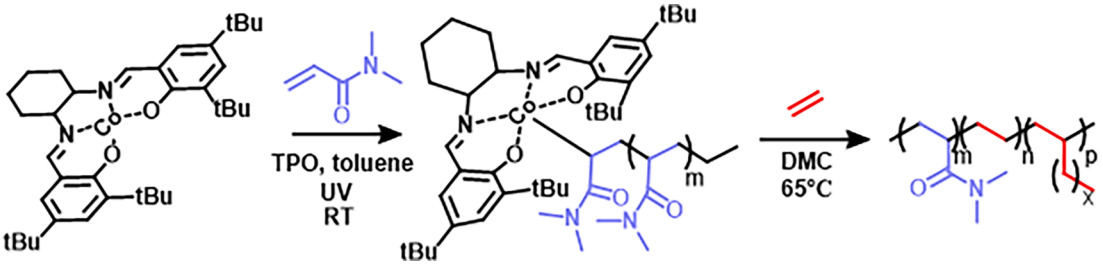


**Scheme 6.** Synthesis of PDMA-*b*-PE copolymers using PMA-Co(Salen) dormant species.

**Table 5**
PDMA-*b*-PE block copolymer by ethylene radical chain extension using PDMA-Co(Salen) dormant species.

| Entry | $Mn_{theo.}^{PDMA}$ (g/mol)[a] | $Mn_{exp.}^{PDMA}$ (g/mol)[b] | Đ[b] | [Py]: [$Co^{II}$] | Pressure (bar) | Time (hr) | $DP_{nmr}$ (PE) [c] | DP(PE)[d] | $Mn_{exp.}^{PDMA-PE}$ (g/mol)[b] | Đ[b] |
|---|---|---|---|---|---|---|---|---|---|---|
| 1 | 8,100 | 10,260 | 1.39 | 0 | 50 | 48 | 3.7 | 4.6 ± 0.1 | 10,630 | 1.40 |
| 2 | 3,000 | 2,200 | 1.34 | 3 | 50 | 48 | 3.8 | 4.4 ± 0.1 | 2,640 | 1.98 |
| 3 | 6,200 | 6,820 | 1.40 | 0 | 50 | 72 | 5.9 | 6.1 ± 0.2 | 7,410 | 1.71 |
| 4 | 3,500 | 3,620 | 1.37 | 3 | 50 | 72 | 7.2 | 7.6 ± 0.3 | 4,850 | 1.57 |
| 5 | 4,800 | 6,060 | 1.37 | 0 | 60 | 48 | 3.9 | 4.9 ± 0.1 | 7,890 | 1.42 |
| 6 | 3,700 | 4,610 | 1.39 | 3 | 60 | 48 | 4.8 | 5.6 ± 0.1 | 5,860 | 1.32 |

[a] The theoretical molecular weight was calculated based on the following equation: $M_n^{theo.\ PDMA} = ([M]_0/[Co(Salen)] \times Mw^{DMA}) \times$ poly(N, N-dimethyl acrylamide) conversion, where $[M]_0$, [Co(Salen)], and $Mw^{DMA}$ correspond to initial monomer concentration, initial Co(Salen) catalyst concentration, and molar mass of the DMA, respectively. [b]The experimental molecular weight ($Mn_{exp}$) and *Đ* were determined by GPC analysis with samples run in DMF containing 10 mmol/L LiBr at 40°C calibrated to poly(methyl methacrylate) standards. [c]The DP(PE) was calculated based on the following equation: DP(PE) = ((Integral (0.8–1.85 ppm)-Integral (1.85–3.5 ppm) ÷ 7 × 2)4)/(Integral (6.6–6.8 ppm)/2 + Integral(7.5–7.8 ppm)/4). [d]The $DP^{cal.}$(PE) was calculated from DP (PE) following the equation $DP^{cal.}$(PE) = DP (PE) ÷ Conversion. The Conversion was the average conversion from the PDMA-Co(Salen) TEMPO trapping experiments (Table S10). The error was calculated from the difference between 2 experiments runs of TEMPO trapping experiments.

observation from the PVAc-*b*-PE copolymer preparation. The $DP^{cal.}$(PE) in regards to the same reaction time, can be modulated through a change of ethylene pressure (Table 5, entries 1–6). These observations were in agreement with the previous study that increasing reaction time and an addition of electron donor led to an increase in PE production together with a higher amount of macroradical generation.

## 3. Conclusion

This work assessed the synthesis of polar-PE block copolymers combining the free radical polymerization of ethylene and OMRP of polar monomers using Co(Salen) to mediate the controlled radical polymerization of MA, VAc, and DMA. The thermal activation using AIBN was investigated to control the radical polymerization of the chosen polar monomers. While it was successful with MA and VAc, an uncontrolled radical polymerization was observed with DMA. The photoinitiated polymerization using TPO under UV irradiation was therefore chosen for the synthesis of polymeric Co(Salen)dormant species. The ability of polymeric Co(Salen) dormant species to reactivate radicals through the RT mechanism, working as macroinitiator, proposes a new pathway to polar polyethylene block copolymers. To validate reactivation from dormant species, we performed TEMPO trapping and propagation resumption experiments. The propagation resumption proved that the dormant species could resume radical polymerization under both thermal activation and photo-irradiation. These experiments confirmed the possibility for dormant species to serve as initiators in thermally initiated free radical polymerization. After successful formation of copolymers by free radical copolymerization, we concluded that a more stabilized radical can initiate a monomer leading to a less stable radical and vice versa. The radical initiation rate of polar macroradicals was quantified by TEMPO trapping experiments as increased reaction times and the presence of electron donors increased the amount of reactivated radicals for consecutive polymerization with ethylene. PMA-*b*-PE, PVAc-*b*-PE, and PDMA-*b*-PE block copolymers were prepared by PMA-Co(Salen), PVAc-Co(Salen), and PDMA-Co(Salen) initiated ethylene polymerization. This work utilized one catalyst and three different radical mechanisms, DT mechanism (preparation of dormant species), RT (reactivation of dormant species) and free radical polymerization (ethylene polymerization) to achieve the synthesis of a diverse set of polar PE block copolymers.

## CRediT authorship contribution statement

**Chenying Zhao:** Writing – review & editing, Writing – original draft, Visualization, Validation, Methodology, Investigation, Formal analysis, Data curation, Conceptualization. **Eva Harth:** Writing – review & editing, Visualization, Validation, Supervision, Software, Resources, Project administration, Methodology, Investigation, Funding acquisition, Formal analysis, Data curation, Conceptualization.

## Declaration of competing interest

The authors declare that they have no known competing financial interests or personal relationships that could have appeared to influence the work reported in this paper.

## Data availability

Data will be made available on request.

## Acknowledgments

The authors C.Z. and E.H. thank the Robert A. Welch Foundation, USA for the generous support of this research (#H-E-0041 and #E-2066-202110327) through the Center of Excellence in Polymer Chemistry. The authors also gratefully acknowledge the National Science Foundation, USA for supporting parts of this work (CHEM-2108576). The authors thank Dr. Steve Swinnea for SAXS measurements at UT Austin.

## Appendix A. Supplementary data

Supplementary data to this article can be found online at https://doi.org/10.1016/j.eurpolymj.2024.113460.

## References

[1] C. Vasile, M. Pascu, Practical guide to polyethylene, iSmithers Rapra Publishing2005.
[2] P. Ehrlich, G.A. Mortimer, Fundamentals of the free-radical polymerization of ethylene, Springer, Fortschritte der Hochpolymeren-Forschung, 2006, pp. 386–448.
[3] S. Mecking, L.K. Johnson, L. Wang, M. Brookhart, Mechanistic Studies of the Palladium-Catalyzed Copolymerization of Ethylene and α-Olefins with Methyl Acrylate, J. Am. Chem. Soc. 120 (5) (1998) 888–899.
[4] L.K. Johnson, S. Mecking, M. Brookhart, Copolymerization of ethylene and propylene with functionalized vinyl monomers by palladium (II) catalysts, J. Am. Chem. Soc. 118 (1) (1996) 267–268.
[5] K. Nozaki, S. Kusumoto, S. Noda, T. Kochi, L.W. Chung, K. Morokuma, Why did incorporation of acrylonitrile to a linear polyethylene become possible? Comparison of phosphine− sulfonate ligand with diphosphine and imine− phenolate ligands in the Pd-catalyzed ethylene/acrylonitrile copolymerization, J. Am. Chem. Soc. 132 (45) (2010) 16030–16042.
[6] A. Kermagoret, A. Debuigne, C. Jérôme, C. Detrembleur, Precision design of ethylene-and polar-monomer-based copolymers by organometallic-mediated radical polymerization, Nat. Chem. 6 (3) (2014) 179–187.
[7] R.S. Faibish, Y. Cohen, Fouling-resistant ceramic-supported polymer membranes for ultrafiltration of oil-in-water microemulsions, J. Membr. Sci. 185 (2) (2001) 129–143.
[8] J. Loste, J.-M. Lopez-Cuesta, L. Billon, H. Garay, M. Save, Transparent polymer nanocomposites: An overview on their synthesis and advanced properties, Prog. Polym. Sci. 89 (2019) 133–158.
[9] J. Critchley, G. Knight, W.W. Wright, Heat-resistant polymers: technologically useful materials, Springer Science & Business Media, 2013.
[10] K.K. Ajekwene, Properties and applications of acrylates, Acrylate Polymers for Advanced Applications 6 (2020) 35–46.

[11] F.S. Bates, G.H. Fredrickson, Block copolymer thermodynamics: theory and experiment, Annu. Rev. Phys. Chem. 41 (1) (1990) 525–557.
[12] F.S. Bates, G.H. Fredrickson, Block Copolymers—Designer Soft Materials, Phys. Today 52 (2) (1999) 32–38.
[13] A. Noshay, J.E. McGrath, Block copolymers: overview and critical survey, (2013).
[14] H. Dau, G.R. Jones, E. Tsogtgerel, D. Nguyen, A. Keyes, Y.-S. Liu, H. Rauf, E. Ordonez, V. Puchelle, H. Basbug Alhan, C. Zhao, E. Harth, Linear Block Copolymer Synthesis, Chemical Reviews 122 (18) (2022) 14471–14553.
[15] B.S. Williams, M.D. Leatherman, P.S. White, M. Brookhart, Reactions of Vinyl Acetate and Vinyl Trifluoroacetate with Cationic Diimine Pd(II) and Ni(II) Alkyl Complexes: Identification of Problems Connected with Copolymerizations of These Monomers with Ethylene, J. Am. Chem. Soc. 127 (14) (2005) 5132–5146.
[16] Z. Saki, I. D'Auria, A. Dall'Anese, B. Milani, C. Pellecchia, Copolymerization of Ethylene and Methyl Acrylate by Pyridylimino Ni(II) Catalysts Affording Hyperbranched Poly(ethylene-co-methyl acrylate)s with Tunable Structures of the Ester Groups, Macromolecules 53 (21) (2020) 9294–9305.
[17] S. Coca, K. Matyjaszewski, Block Copolymers by Transformation of "Living" Carbocationic into "Living" Radical Polymerization, Macromolecules 30 (9) (1997) 2808–2810.
[18] C.J. Kay, P.D. Goring, C.A. Burnett, B. Hornby, K. Lewtas, S. Morris, C. Morton, T. McNally, G.W. Theaker, C. Waterson, Polyolefin–polar block copolymers from versatile new macromonomers, J. Am. Chem. Soc. 140 (42) (2018) 13921–13934.
[19] S.M. Stadler, I. Göttker-Schnetmann, A.S. Fuchs, S.R.R. Fischer, S. Mecking, Catalytic Chain Transfer Polymerization to Functional Reactive End Groups for Controlled Free Radical Growth, Macromolecules 53 (7) (2020) 2362–2368.
[20] H. Dau, E. Tsogtgerel, K. Matyjaszewski, E. Harth, One-For-All Polyolefin Functionalization: Active Ester as Gateway to Combine Insertion Polymerization with ROP, NMP, and RAFT, Angew. Chem. Int. Ed. 134 (33) (2022) e202205931.
[21] A. Keyes, H. Dau, K. Matyjaszewski, E. Harth, Tandem Living Insertion and Controlled Radical Polymerization for Polyolefin–Polyvinyl Block Copolymers, Angew. Chem. Int. Ed. (2021) e202112742.
[22] A. Keyes, H.E. Basbug Alhan, U. Ha, Y.-S. Liu, S.K. Smith, T.S. Teets, D.B. Beezer, E. Harth, Light as a Catalytic Switch for Block Copolymer Architectures: Metal-Organic Insertion/Light Initiated Radical (MILRad) Polymerization, Macromolecules 51 (18) (2018) 7224–7232.
[23] W.-C. Lin, W. Fan, A. Marcellan, D. Hourdet, C. Creton, Large Strain and Fracture Properties of Poly(dimethylacrylamide)/Silica Hybrid Hydrogels, Macromolecules 43 (5) (2010) 2554–2563.
[24] F. Baffie, G. Patias, A. Shegiwal, F. Brunel, V. Monteil, L. Verrieux, L. Perrin, D. M. Haddleton, F. D'Agosto, Block Copolymers Based on Ethylene and Methacrylates Using a Combination of Catalytic Chain Transfer Polymerisation (CCTP) and Radical Polymerisation, Angew. Chem. Int. Ed. 60 (48) (2021) 25356–25364.
[25] C. Bergerbit, F. Baffie, A. Wolpers, P.Y. Dugas, O. Boyron, M. Taam, M. Lansalot, V. Monteil, F. d'Agosto, Ethylene Polymerization-Induced Self-Assembly (PISA) of Poly (ethylene oxide)-block-polyethylene Copolymers via RAFT, Angew. Chem. Int. Ed. 132 (26) (2020) 10471–10476.
[26] B.C. Qian, L. Zhang, G.S. Zhang, Y.H. Fu, X.Q. Zhu, G.B. Shen, Thermodynamic Evaluation on Alkoxyamines of TEMPO Derivatives, Stable Alkoxyamines or Potential Radical Donors? ChemistrySelect 7 (45) (2022) e202204144.
[27] J. Demarteau, A. Debuigne, C. Detrembleur, Organocobalt Complexes as Sources of Carbon-Centered Radicals for Organic and Polymer Chemistries, Chem. Rev. 119 (12) (2019) 6906–6955.
[28] R. Poli, Relationship Between One-Electron Transition-Metal Reactivity and Radical Polymerization Processes, Angew. Chem. Int. Ed. 45 (31) (2006) 5058–5070.
[29] M.B. Gillies, K. Matyjaszewski, P.-O. Norrby, T. Pintauer, R. Poli, P. Richard, A DFT study of R− X bond dissociation enthalpies of relevance to the initiation process of atom transfer radical polymerization, Macromolecules 36 (22) (2003) 8551–8559.
[30] Y. Nakamura, B. Ebeling, A. Wolpers, V. Monteil, F. D'Agosto, S. Yamago, Controlled Radical Polymerization of Ethylene Using Organotellurium Compounds, Angew. Chem. Int. Ed. 57 (1) (2018) 305–309.
[31] A. Wolpers, C. Bergerbit, B. Ebeling, F. d'Agosto, V. Monteil, Aromatic xanthates and dithiocarbamates for the polymerization of ethylene through reversible addition–fragmentation chain transfer (RAFT), Angew. Chem. Int. Ed. 58 (40) (2019) 14295–14302.
[32] J. Demarteau, P.B. Scholten, A. Kermagoret, J. De Winter, M.A. Meier, V. Monteil, A. Debuigne, C. Detrembleur, Functional polyethylene (PE) and PE-based block copolymers by organometallic-mediated radical polymerization, Macromolecules 52 (22) (2019) 9053–9063.
[33] A. Debuigne, R. Poli, C. Jérôme, R. Jérôme, C. Detrembleur, Overview of cobalt-mediated radical polymerization: Roots, state of the art and future prospects, Prog. Polym. Sci. 34 (3) (2009) 211–239.
[34] C.-H. Peng, J. Scricco, S. Li, M. Fryd, B.B. Wayland, Organo-Cobalt Mediated Living Radical Polymerization of Vinyl Acetate, Macromolecules 41 (7) (2008) 2368–2373.
[35] M. Hurtgen, A. Debuigne, C. Jérôme, C. Detrembleur, Solving the problem of bis (acetylacetonato) cobalt (II)-mediated radical polymerization (CMRP) of acrylic esters, Macromolecules 43 (2) (2010) 886–894.
[36] M. Hurtgen, J. Liu, A. Debuigne, C. Jerome, C. Detrembleur, Synthesis of thermo-responsive poly(N-vinylcaprolactam)-containing block copolymers by cobalt-mediated radical polymerization, Polym. Chem. 50 (2) (2012) 400–408.
[37] R. Poli, New Phenomena in Organometallic-Mediated Radical Polymerization (OMRP) and Perspectives for Control of Less Active Monomers, Eur. J. Chem. 21 (19) (2015) 6988–7001.
[38] C.-M. Liao, C.-C. Hsu, F.-S. Wang, B.B. Wayland, C.-H. Peng, Living radical polymerization of vinyl acetate and methyl acrylate mediated by Co (Salen*) complexes, Polym. Chem. 4 (10) (2013) 3098–3104.
[39] Y. Zhao, S. Zhang, Z. Wu, X. Liu, X. Zhao, C.-H. Peng, X. Fu, Visible-light-induced living radical polymerization (LRP) mediated by (Salen) Co (II)/TPO at ambient temperature, Macromolecules 48 (15) (2015) 5132–5139.
[40] C.-S. Hsu, T.-Y. Yang, C.-H. Peng, Vinyl acetate living radical polymerization mediated by cobalt porphyrins: kinetic–mechanistic studies, Polym. Chem. 5 (12) (2014) 3867–3875.
[41] L.F. Oliveira, C. Bignardi, N.M. Pesqueira, B.A. Riga–Rocha, A.E. Machado, V.P. Carvalho–Jr, B.E. Goi, Photocontrolled reversible-deactivation radical polymerization of butyl acrylate mediated by Salen-type CoII complexes, Eur. Polym. J. 159 (2021) 110757.
[42] A. Debuigne, J.-R. Caille, R. Jérôme, Synthesis of end-functional poly (vinyl acetate) by cobalt-mediated radical polymerization, Macromolecules 38 (13) (2005) 5452–5458.
[43] E. Grau, J.-P. Broyer, C. Boisson, R. Spitz, V. Monteil, Free ethylene radical polymerization under mild conditions: the impact of the solvent, Macromolecules 42 (19) (2009) 7279–7281.
[44] E. Grau, J.-P. Broyer, C. Boisson, R. Spitz, V. Monteil, Unusual activation by solvent of the ethylene free radical polymerization, Polym. Chem. 2 (10) (2011) 2328–2333.
[45] Y. Wang, Y. Zhao, S. Zhu, X. Zhou, J. Xu, X. Xie, R. Poli, Switchable polymerization triggered by fast and quantitative insertion of carbon monoxide into cobalt–oxygen bonds, Angew. Chem. Int. Ed. 132 (15) (2020) 6044–6050.
[46] T. Fukuda, K. Kubo, Y.-D. Ma, Kinetics of free radical copolymerization, Prog. Polym. Sci. 17 (5) (1992) 875–916.
[47] J. Eguiburu, J. Iruin, M. Fernandez-Berridi, J. San Román, Blends of amorphous and crystalline polylactides with poly (methyl methacrylate) and poly (methyl acrylate): a miscibility study, Polymer 39(26) (1998) 6891-6897.
[48] H. Sasabe, C.T. Moynihan, Structural relaxation in poly (vinyl acetate), J. Polym. Sci., Polym. Phys. Ed. 16(8) (1978) 1447-1457.
[49] M. Ribeiro E Silva, J.C. Machado, V. Mano, G.G. Silva, Positron annihilation and differential scanning calorimetry studies of polyacrylamide and poly (dimethylacrylamide)/poly (ethylene glycol) blends, J. Polym. Sci., Part B: Polym. Phys. 41(13) (2003) 1493-1500.
[50] S. Maria, H. Kaneyoshi, K. Matyjaszewski, R. Poli, Effect of Electron Donors on the Radical Polymerization of Vinyl Acetate Mediated by [Co(acac)2]: Degenerative Transfer versus Reversible Homolytic Cleavage of an Organocobalt(III) Complex, Eur. J. Chem. 13 (9) (2007) 2480–2492.